

Application of the effective Fisher matrix to the frequency domain inspiral waveforms

Hee-Suk Cho¹ and Chang-Hwan Lee¹

¹*Department of Physics, Pusan National University, Busan 609-735, Korea*

(Dated: March 20, 2014)

The Fisher matrix (FM) has been generally used to predict the accuracy of the gravitational wave parameter estimation. Although a limitation of the FM has been well known, it is still mainly used due to its very low computational cost compared to the Monte Carlo simulations. Recently, Rodriguez *et al.* performed Markov chain Monte Carlo (MCMC) simulations for nonspinning binary systems with total masses $M \leq 20M_\odot$, they found systematic differences between the predictions from FM and MCMC for $M > 10M_\odot$. On the other hand, an effective Fisher matrix (eFM) was recently introduced by Cho *et al.* The eFM is a semi-analytic approach to the standard FM, in which the partial derivative is taken by a quadratic fitting function to the local overlap surface. In this letter, we apply the eFM method to several nonspinning binary systems and find that the error bounds in eFM are qualitatively in good agreement with the MCMC results. In particular, we give a convincing explanation on that the inconsistency between the FM and MCMC in high mass region is mainly caused by the template-independent frequency cutoff of the inspiral waveforms.

PACS numbers: 04.30.-w, 04.80.Nn, 95.55.Ym

In ground-based gravitational wave data analysis, various parameter estimation methods are implemented to find the physical parameters of the gravitational wave sources. One of the most promising techniques is the Markov chain Monte Carlo (MCMC) [1–6], which involves the Bayesian analysis framework. The MCMC enables us to search the whole parameter space within given templates and find the physical parameters from the wave signal and the error bounds on their variances. The Fisher matrix (FM) has been generally used to estimate the error bounds [7–10]. Despite the well-known limitations, the FM method is being used because it is quite easy to use and needs very low computational cost compared to the Monte Carlo simulations. Several studies investigated the inconsistencies between the FM and the Monte Carlo methods [1, 11, 12], especially, Rodriguez *et al.* [12] (henceforth denoted RFFM) performed a systematic comparison between the FM error estimates and the MCMC probability density functions using plenty of nonspinning binary systems with component masses in $1M_\odot \leq m_1, m_2 \leq 15M_\odot$ and total masses in $M \leq 20M_\odot$. They found that the FM overestimates the uncertainty in the parameter estimation achievable by the MCMC in high mass region, and the disagreement increases with total mass. They explored a variety of possibilities but have not been able to find convincing explanations for the inconsistency.

On the other hand, an effective Fisher matrix (eFM) was recently developed by Cho *et al.* [13]. They showed a good agreement between the eFM and MCMC uncertainty predictions of mass parameters using a time domain inspiral waveform for a black hole-neutron star binary with masses of $10M_\odot$ and $1.4M_\odot$ [5, 6]. While the FM computation is based on differentiating a waveform with respect to its parameters at the maximum overlap point, the eFM calculates the derivative by a fitting func-

tion to the local overlap surface surrounding the maximum point. If the infinitesimal region at the maximum point well-represents the Gaussian likelihood surface of the MCMC, these two methods are formally consistent and both will give a good estimate of the MCMC probability density function. In this letter, we apply the eFM method to several nonspinning binary systems with the same mass ranges as in RFFM. We compute the standard deviations of mass parameters and compare with those of FM (the result is summarized in Fig. 2). We find the divergent trend in fractional differences is consistent with that of RFFM, and the error bounds in eFMs are qualitatively in good agreement with the MCMC predictions. From our detailed numerical approach we confirm that the inconsistency in high mass region is mainly caused by the template-independent frequency cutoff of the inspiral waveforms. We show that the eFM method can overcome this problem by semi-analytically differentiating the *accurate* overlap surface which incorporates the template-dependent frequency cutoff. Throughout this letter, all mass parameters are in units of the solar mass (M_\odot) unless otherwise noticed, and we use a geometrized unit, where $G = c = 1$.

We use the TaylorF2 waveform that is implemented in the LIGO Algorithm Library [14]. TaylorF2 model is currently available up to 3.5 pN order in phase, but we only consider 2 pN waveform for consistency with the MCMC simulations in RFFM. The analytic function of TaylorF2 waveform is given by

$$\tilde{h}(f) = Af^{-7/6}e^{i\Psi(f)}, \quad (1)$$

where the wave amplitude (A) consists of the binary masses and five extrinsic parameters, i.e., the luminosity distance of the binary, the sky position (RA, DEC), the orbital inclination, and the wave polarization. For simplicity, we assume an optimally located binary system as in [13] and a fixed signal-to-noise ratio

(SNR), then all information of the waveform is determined by the pN phase (Ψ) which consists of the chirp mass ($M_c = m_1^{3/5} m_2^{3/5} M^{-1/5}$), symmetric mass ratio ($\eta = m_1 m_2 M^{-2}$), coalescence time (t_c), and coalescence phase (ϕ_c). Hence, we only consider these four parameters in FM. Generally, since the extrinsic parameters are nearly uncorrelated with the four parameters [12], removing the extrinsic parameters from the 9×9 FM will not affect the 4×4 covariance matrix consisting of $\{M_c, \eta, t_c, \phi_c\}$. The low frequency limit for generation of waveform is fixed to be 40 Hz for both signal and template to be consistent with the initial LIGO noise sensitivity curve [15]. The maximum frequency cutoff (f_{\max}) is taken when the binary hits the “innermost-stable-circular orbit (ISCO)”, that is defined as a function of the total mass ($M = m_1 + m_2$) of the system:

$$f_{\max} = f_{\text{ISCO}} = \frac{1}{6^{3/2} \pi M}. \quad (2)$$

The FM for a waveform $\tilde{h}(\lambda)$ is defined by

$$\Gamma_{ij} = \left\langle \frac{\partial \tilde{h}}{\partial \lambda_i} \left| \frac{\partial \tilde{h}}{\partial \lambda_j} \right. \right\rangle \Big|_{\lambda=\lambda_0}, \quad (3)$$

where λ_0 is the true value of each parameter and $\lambda_i = \{M_c, \eta, \phi_c, t_c\}$. Since the pN phase of the TaylorF2 is an analytic function of the parameters, the derivative can be obtained analytically. The overlap between a signal (\tilde{h}_s) and a template (\tilde{h}_t) is defined by

$$\langle \tilde{h}_s | \tilde{h}_t \rangle = 4 \text{Re} \int_0^\infty \frac{\tilde{h}_s(f) \tilde{h}_t^*(f)}{S_n(f)} df. \quad (4)$$

Note that the inverse Fourier transform will compute the overlap for all possible coalescence times at once [16]. In addition, by taking the absolute value of the complex number we can maximize the overlap over all possible coalescence phases [16]. Here, as noted in [17], one should be confident that the true maximum is never missed in the sufficiently small tolerance level for the maximizing algorithm. To do this, we apply a nearly continuous time shift by reducing a step size when performing the inverse fast Fourier transform. We found that, for $dt \sim 10^{-5}$ s, all numerical errors in this work can be neglected.

The inconsistency between FM and MCMC was first noted by [1], and robustly confirmed by RFFM from plenty of simulations. The former [1] showed that allowing the templates in MCMC to have $\eta > 0.25$ partially reduced the discrepancy between the FM and MCMC for symmetric mass systems. In RFFM, the authors also explored various possibilities but could not find a convincing explanation on the discrepancy. On the other hand, another possibility caused by sharp frequency cutoff of the inspiral waveform was shortly mentioned by [1], and [18] briefly discussed the importance of this template-dependent frequency cutoff in computing the difference

between two waveforms. An attempt to include this effect in FM was recently performed by [19] by substituting the waveform with the *modified* waveform (\tilde{h}') given by

$$\tilde{h}'(f) = A f^{-7/6} e^{i\Psi(f)} H(f_{\text{ISCO}} - f), \quad (5)$$

where H is the Heaviside step function. In this case, however, as pointed out by the authors therein, since the computation of the partial derivative must include the delta functions that are not square-integrable, the *modified*-FM with modified waveform cannot be obtained analytically. They also pointed out that the valid mass region of the FM depends on where the inspiral waveform has been terminated in the detector’s noise spectrum. For binaries with $M < 10M_\odot$, f_{ISCO} is sufficiently high such that it is out of band and the H term can be neglected in computing the FM. On the contrary, for more massive binaries, f_{ISCO} is placed in the sensitivity band and the H term becomes non-negligible. They claimed that this is why RFFM obtained an apparent violation of the error bound with the FM for more massive systems but not for the low mass ones.

In summary, when using the inspiral-only waveforms the FM is valid only when the binary mass is less than $10M_\odot$. For higher mass binaries, one additional term should be included in the wave function to incorporate the template-dependent frequency cutoff. In this case, however, the analytical approach fails to estimate the accurate error bounds because the *modified*-FM is analytically incomputable.

However, in MCMC formalism, the posteriors can be obtained without any singular behavior because the MCMC treats the template-dependent frequency cutoff numerically. In order to estimate the likelihood distributions of MCMC, we investigate the overlap surface in detail. If we define the normalized overlap by

$$P(\tilde{h}_s, \tilde{h}_t) = \frac{\langle \tilde{h}_s | \tilde{h}_t \rangle}{\sqrt{\langle \tilde{h}_s | \tilde{h}_s \rangle \langle \tilde{h}_t | \tilde{h}_t \rangle}}, \quad (6)$$

the log likelihood ($\ln L$) of MCMC can be expressed by [13],

$$\ln L(\lambda) = -\rho^2(1 - P), \quad (7)$$

where ρ is the SNR. We assume a template h_t and a signal h_s with total masses M_t and M_s , and denote each frequency cutoff by f_{\max}^t and f_{\max}^s . To test the cutoff dependence, one can consider two different cases.

(i) **Template-independent frequency cutoff :**

If we fix the frequency cutoff of the template to be the same as f_{\max}^s independently of the total mass of the template, the overlap in Eq. (6) becomes simply

$$P_{\text{TI}} = \frac{\langle \tilde{h}_s | \tilde{h}_t \rangle|_0^{f_{\max}^s}}{\sqrt{\langle \tilde{h}_s | \tilde{h}_s \rangle|_0^{f_{\max}^s} \langle \tilde{h}_t | \tilde{h}_t \rangle|_0^{f_{\max}^s}}}, \quad (8)$$

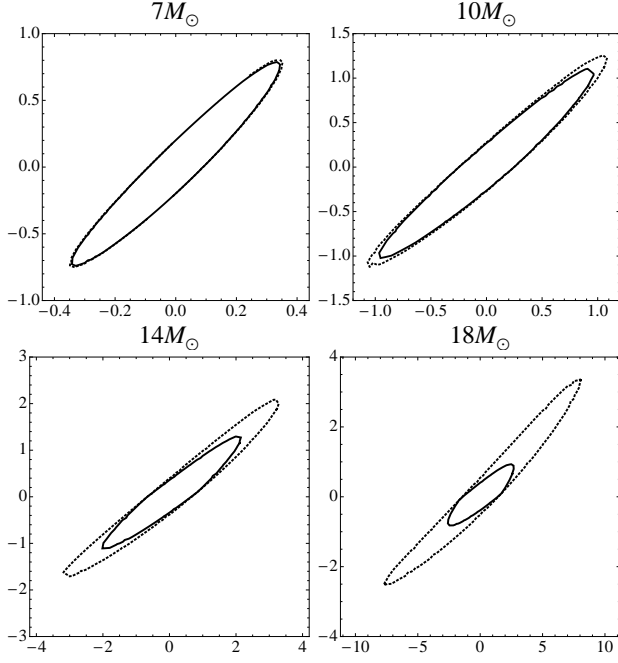


FIG. 1: Comparison between two overlap surfaces with various total masses. In each plot, the horizontal (vertical) axis denotes $\delta M_c (\delta \eta) \times 100$. The contours indicate $P = 0.995$. Solid and dotted lines correspond to the P_{TD} and P_{TI} , respectively. The total mass is denoted in each plot and the mass ratio (m_2/m_1) is $1/4$ for all cases. Note that the difference between two overlap contours is more distinguishable for more massive total masses.

where “ $|^b_a$ ” means the overlap integration should be performed only in the frequency range from a to b .

(i) **Template-dependent frequency cutoff :**

In real overlap computations, such as in MCMC, f_{\max}^t is not fixed but dependent on the template mass, so generally $f_{\max}^t \neq f_{\max}^s$. In this case the overlap should be

$$P_{TD} = \frac{\langle \tilde{h}_s | \tilde{h}_t \rangle_0^{\min(f_{\max}^t, f_{\max}^s)}}{\sqrt{\langle \tilde{h}_s | \tilde{h}_s \rangle_0^{f_{\max}^s} \langle \tilde{h}_t | \tilde{h}_t \rangle_0^{f_{\max}^t}}}. \quad (9)$$

where $\langle \tilde{h}_s | \tilde{h}_s \rangle$ is independent of the template, hence always the same as that in P_{TI} . If $f_{\max}^t > f_{\max}^s$, then the numerator $\langle \tilde{h}_s | \tilde{h}_t \rangle$ is also the same but $\langle \tilde{h}_t | \tilde{h}_t \rangle$ in the denominator should be larger than that in P_{TI} , consequently $P_{TD} < P_{TI}$. On the contrary, if $f_{\max}^t < f_{\max}^s$, then both $\langle \tilde{h}_s | \tilde{h}_t \rangle$ and $\langle \tilde{h}_t | \tilde{h}_t \rangle$ should be smaller but the numerator decreases more rapidly than the denominator, hence again $P_{TD} < P_{TI}$.

There exists non vanishing difference between the two overlaps ($\Delta P = P_{TI} - P_{TD}$) when $f_{\max}^t \neq f_{\max}^s$, which turns out to be very important as the total mass increases. To see a contribution rate of ΔP to the overlap

integration, we show the overlap contours for both P_{TI} and P_{TD} with various total masses in Fig. 1. One can see that the overlap contours are more broad for P_{TI} , and the difference between the two overlaps is more distinguishable for more massive total masses.

The FM can be directly derived by the log likelihood ($\ln L$) [13, 20, 21], then from Eq. (7) we have

$$\Gamma_{ij} = -\frac{\partial^2 \ln L(\lambda)}{\partial \lambda_i \partial \lambda_j} = \rho^2 \frac{\partial^2 (1-P)}{\partial \lambda_i \partial \lambda_j} \Big|_{\lambda=\lambda_0}. \quad (10)$$

In this expression the overlap is not an analytic function, hence, we have to calculate the partial derivative numerically. However, since the likelihood can be expressed by a Gaussian distribution in the limit of high SNR, a multivariate quadratic function best fits the local overlap surface. So if we find an analytic fitting function F to the overlap P at the physically acceptable fitting regions, the derivative can be analytically obtained. Using this function, Cho *et al.* [13] defined the eFM by

$$\Gamma_{\text{eff}} = -\frac{\partial^2 F(\lambda)}{\partial \lambda_i \partial \lambda_j} \Big|_{\lambda=\lambda_0}. \quad (11)$$

In this work, we choose the fitting region as $P > 0.995$ (see Fig. 3 and Cho *et al.* [13] for details).

By applying the eFM method to the overlap P_{TD} , one can access the *modified*-FM numerically. We explore various nonspinning binary models with the same mass ranges as in RFFM. For three different values of the input mass ratio, $m_2/m_1 = \{1/10, 1/4, 1/2\}$ (i.e., $\eta = \{0.09, 0.16, 0.22\}$), we compare the eFM with the FM in the same way as in RFFM, showing the fractional differences between the FM and eFM standard deviations,

$$\Lambda \equiv \frac{\sigma^{\text{FM}}}{\sigma^{\text{eFM}}}. \quad (12)$$

Our results are summarized in Fig. 2. The FM and eFM results are in good agreement with total masses below $10M_\odot$ for both M_c and η . However, as the total mass increases, the fractional differences also monotonically increase, the FM overestimates the eFM standard deviations by a factor of 5 in M_c , and 8 in η at high masses ($\sim 20M_\odot$). We find the overall trend in this result is consistent with that of RFFM (see, Fig. 1, therein), and the eFM predictions are qualitatively in good agreement with the MCMC results. Although we did not perform a direct comparison between the eFM and MCMC, this result indicates that the eFM can dramatically overcome the indeterminacy of the analytic *modified*-FM in high mass region by exploring the *accurate* overlap surface numerically. In this work, we only considered sufficiently asymmetric binaries with $m_2/m_1 \leq 1/2$, because in RFFM the majority of their signals (i.e., 65 % over 200 simulations) were selected with sufficiently asymmetric mass ratio such that the $1-\sigma$ surface about the injected values

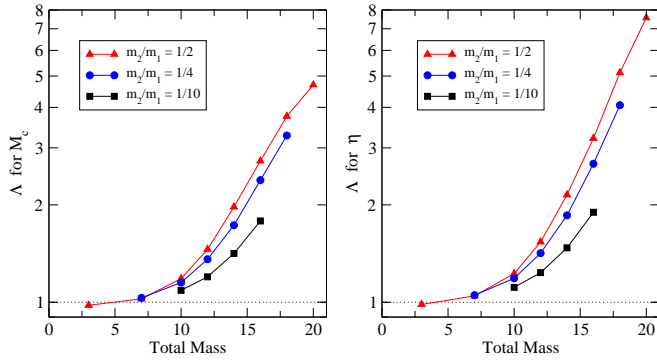


FIG. 2: The fractional difference between the FM and eFM standard deviations as a function of total mass. Note the systematic divergence at $M > 10M_\odot$ for both mass parameters. This trend is consistent with results in RFFM, showing a good agreement between the eFM and MCMC standard deviations qualitatively.

returned by the FM did not exceed the physical boundary $\eta = 0.25$. While RFFM did not give any information of η -dependence on the fractional difference Λ , our result shows that the divergent trend of Λ is more pronounced for more symmetric binaries. It would be interesting to check this η -dependence using the MCMC simulations in RFFM.

Finally, we briefly discuss the accuracy and limitation of our numerical scheme. If we reduce the fitting region, eFM should be consistent with the FM because both methods are formally almost the same. We show a concrete example in Fig. 3, where we calculate the eFM for both cases of template-dependent f_{\max} (P_{TD}) and template-independent f_{\max} (P_{TI}) using a binary with masses of $16M_\odot$ and $4M_\odot$. First, the lower thin lines are obtained by P_{TI} . One can see that the Λ approaches unity without any fluctuations independently of the fitting region. This behavior indicates that unlike the *modified*-FM, the FM is analytically stable and our numerical scheme is working properly to approximate the FM. Second, the upper thick lines are obtained by P_{TD} . In this case, however, the Λ increases with P_{\min} and the fitting region is related with the SNR as $1 - P_{\min} \sim 1/\rho^2$ in our eFM approach [13]. This implies that the effect of the template-independent frequency cutoff can be significant even for the low mass systems if the SNR is sufficiently high. On the other hand, the Λ tends to fluctuate from $P_{\min} = 0.998$ because of the limitation of our numerical precision. Beyond this region, we cannot determine the eFM accurately, hence cannot approximate the analytic *modified*-FM. Note that the eFMs in Fig. 2 were obtained at the stable fitting region, $P > 0.995$ (i.e., $P_{\min} = 0.995$ in Fig. 3).

In this letter, we reviewed the inadequacy of the FM for the inspiral waveforms. The mass range where the FM is valid depends on the detector sensitivity spectrum, the valid range is $M < 10M_\odot$ for the initial LIGO sensitiv-

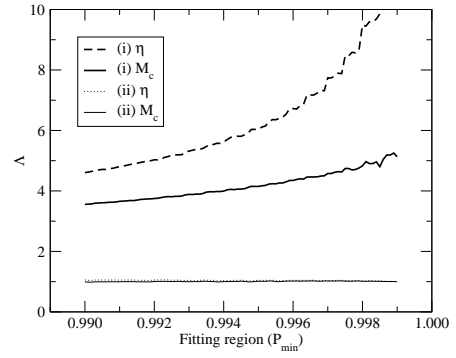


FIG. 3: The fractional difference between the FM and eFM standard deviations as a function of fitting region. We use the binary with component masses of $16M_\odot$ and $4M_\odot$. P_{\min} indicates that the fitting region is $P > P_{\min}$. The upper thick (lower thin) lines are obtained by P_{TD} (P_{TI}). The lower thin lines approach unity without any fluctuations, indicating that the FM is stable and our numerical scheme is working well. The upper thick lines increase with P_{\min} and tend to fluctuate from $P_{\min} = 0.998$, beyond this our numerical scheme is no more valid.

ity. It was found that the inconsistency between the FM and MCMC for the high mass systems is mainly caused by neglecting the template-dependent frequency cutoff of the inspiral waveforms. The *modified*-FM, where the additional term is included to incorporate the template-dependent frequency cutoff, is analytically incomputable. In this work, we provided a convincing explanation on the influence of the template-dependent frequency cutoff on the MCMC posterior by comparing two overlap surfaces. We applied the eFM to various nonspinning binary models and found that the eFM can overcome the indeterminacy of the analytic *modified*-FM by exploring the *accurate* overlap surface numerically, and the error bounds in eFMs were qualitatively in good agreement with the MCMC predictions in all mass ranges. Recently, O'Shaughnessy *et al.* [5, 6] showed a good agreement between the eFM and MCMC using a time domain inspiral waveform for a black hole-neutron star binary with masses of $10M_\odot$ and $1.4M_\odot$. It would be interesting to investigate the consistency for more massive systems.

This study was financially supported by the 2013 Post-Doc. Development Program of Pusan National University. H. S. C. and C. H. L. are supported in part by the National Research Foundation Grant funded by the Korean Government (No. NRF-2011-220-C00029) and the BAERI Nuclear R & D program (No. M20808740002) of Korea.

-
- [1] N. J. Cornish and E. K. Porter, *Class. Quantum Grav.* **23**, S761 (2006).
 - [2] M. van der Sluys, I. Mandel, V. Raymond, V. Kalogera,

- C. Röver, and N. Christensen, *Class. Quantum Grav.* **26**, 204010 (2009).
- [3] N. Cornish, L. Sampson, N. Yunes, and F. Pretorius, *Phys. Rev. D* **84**, 062003 (2011).
- [4] J. Veitch, I. Mandel, B. Aylott, B. Farr, V. Raymond, C. Rodriguez, M. van der Sluys, V. Kalogera, and A. Vecchio, *Phys. Rev. D* **85**, 104045 (2012).
- [5] R. O’Shaughnessy, B. Farr, E. Ochsner, H. -S. Cho, C. Kim, and C. -H. Lee, (arXiv:1308.4704) (2014).
- [6] R. O’Shaughnessy, B. Farr, E. Ochsner, H. -S. Cho, C. Kim, V. Raymond, and C. -H. Lee, (arXiv:1403.0544) (2014).
- [7] E. Poisson and C. M. Will, *Phys. Rev. D* **52**, 848 (1995).
- [8] K. G. Arun, B. R. Iyer, B. S. Sathyaprakash, and P. A. Sundararajan, *Phys. Rev. D* **71**, 084008 (2005).
- [9] R. N. Lang and S. A. Hughes, *Phys. Rev. D* **74**, 122001(2006).
- [10] C. Van den Broeck and A. S. Sengupta, *Class. Quantum Grav.* **24**, 1089 (2007).
- [11] T. Cokelaer, *Class. Quantum Grav.* **25**, 184008 (2008).
- [12] C. L. Rodriguez, B. Farr, W. M. Farr, and I. Mandel, (arXiv:1308.1397) (2013).
- [13] H. -S. Cho, E. Ochsner, R. O’Shaughnessy, C. Kim, and C. -H. Lee, *Phys. Rev. D* **87**, 024004 (2013).
- [14] <https://www.lsc-group.phys.uwm.edu/daswg/projects/lal/night>
- [15] T. Damour, B. R. Iyer, and B. S. Sathyaprakash, *Phys. Rev. D* **63**, 044023 (2001).
- [16] B. Allen, W. G. Anderson, P. R. Brady, D. A. Brown and J. D. E. Creighton, *Phys. Rev. D* **85**, 122006 (2012).
- [17] P. Ajith and S. Bose, *Phys. Rev. D* **79**, 084032 (2009).
- [18] F. Ohme, A. B. Nielsen, D. Keppel, and A. Lundgren, *Phys. Rev. D* **88**, 042002 (2013).
- [19] I. Mandel, W. M. Farr, S. Fairhurst, and C. Berry, LIGO Document P1300222-v1 (2013).
- [20] P. Jaranowski and A. Królak, *Phys. Rev. D* **49**, 1723 (1994).
- [21] M. Vallisneri, *Phys. Rev. D* **77**, 042001 (2008).